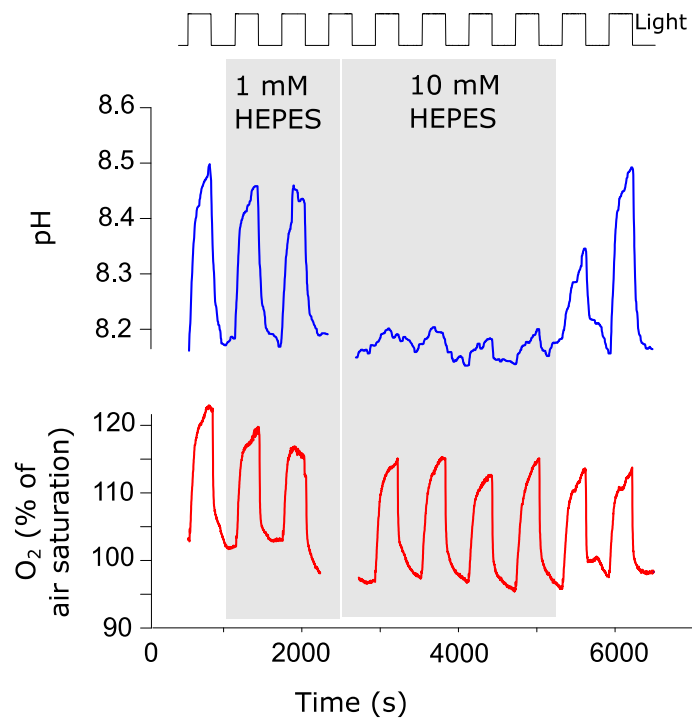


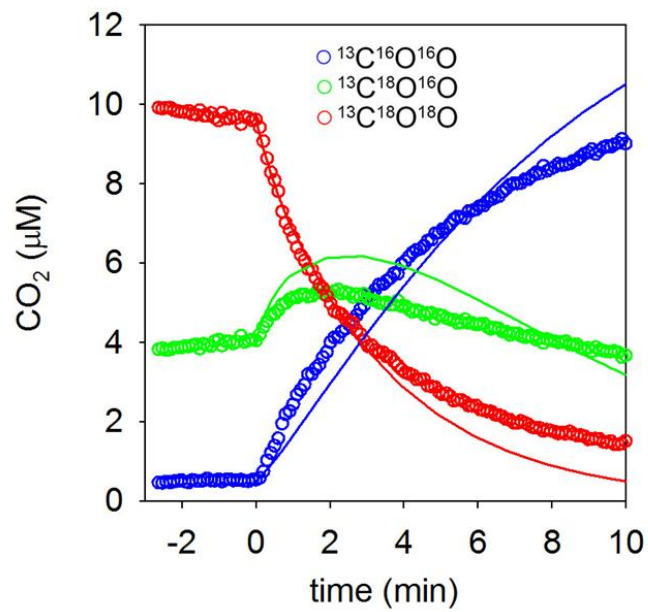
**Supplementary Figure 1: Distribution of chloroplasts in *O. sinensis***

Confocal microscopy of an *O. sinensis* cell indicates that chloroplasts are evenly distributed along the length of the cell. A 3D projection of chlorophyll fluorescence is shown, generated from a Z-stack of 30 images (1  $\mu\text{m}$  per slice). Scale bar represents 100  $\mu\text{m}$ .



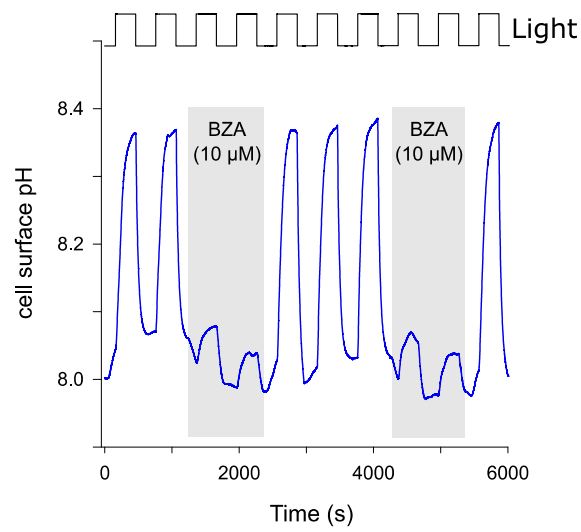
### Supplementary Figure 2: The effects of buffers on cell surface pH

Light-dependent changes in cell surface pH and [O<sub>2</sub>] were measured around an *O. sinensis* cell in normal unbuffered ASW media, ASW + 1 mM HEPES and ASW + 10 mM HEPES (all at pH 8.2). The addition of 10 mM HEPES almost completely buffers the light-dependent increases in cell surface pH, although there is little impact in photosynthetic O<sub>2</sub> evolution. The trace shown is representative of 10 individual cells examined.



**Supplementary Figure 3: Estimation of eCA activity in *O. sinensis* using MIMS**

The removal of <sup>18</sup>O from labelled CO<sub>2</sub> and HCO<sub>3</sub><sup>-</sup> is accelerated upon the addition of *O. sinensis* cells at t=0. The lines show a model fit to the data used to infer absolute eCA activity from <sup>18</sup>O removal dynamics.



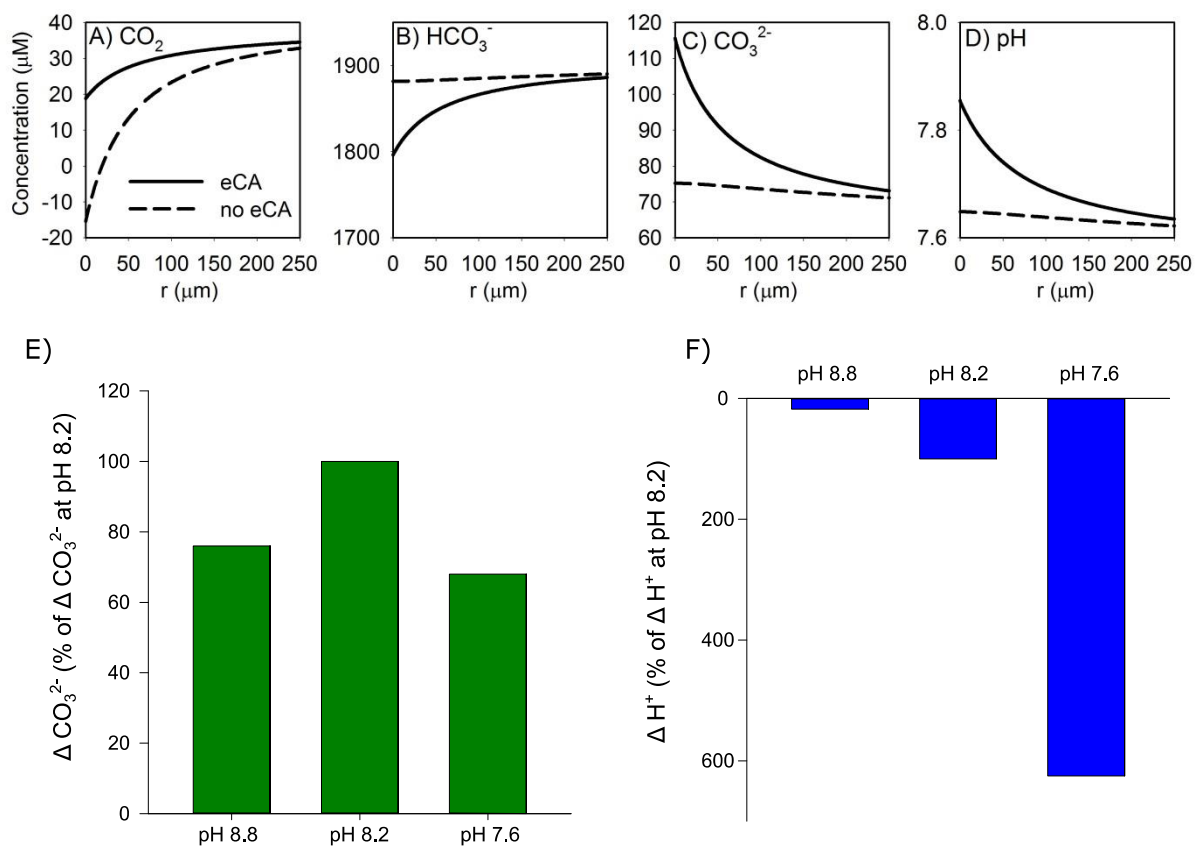
**Supplementary Figure 4: Inhibition of eCA by benzolamide.**

Rapid inhibition of the light-dependent increase in cell surface pH in *O. sinensis* by 10 μM benzolamide (BZA). pH was monitored at the surface of a single *O. sinensis* cell. The effect of 10 μM BZA was reversible, with all cells exhibiting a rapid recovery from inhibition. The trace shown is representative of 8 cells examined.



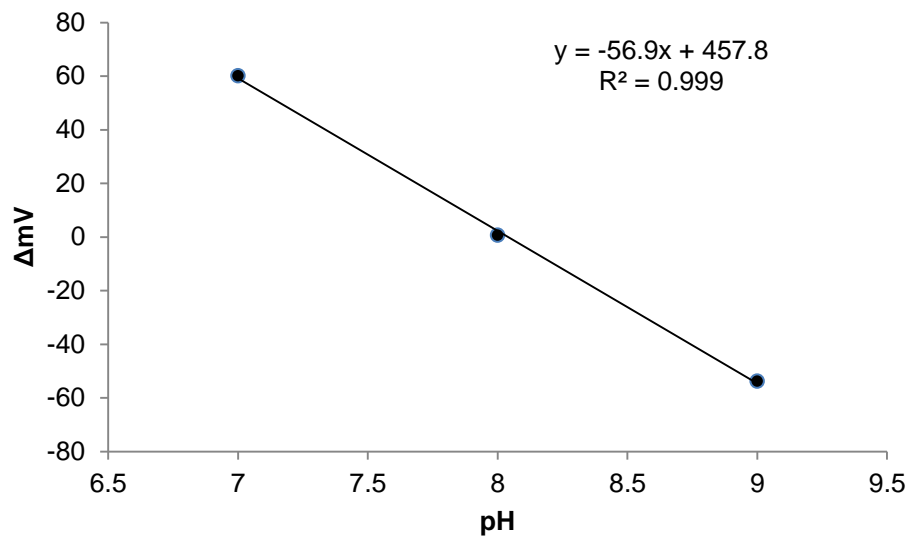
**Supplementary Figure 5: Positioning of microelectrodes around an *O. sinensis* cell for simultaneous measurement of pH and  $\text{CO}_3^{2-}$**

Custom-made microelectrodes were positioned using micromanipulators against the frustule in the central region of an *O. sinensis* cell. For simultaneous measurement of pH and  $[\text{CO}_3^{2-}]$ , the respective ion-selective microelectrodes were positioned on opposing sides of the cell, which had the added benefit of stabilising the cell. The image shows blunt-ended microelectrodes that were used with the larger diatom species (*O. sinensis* and *Coscinodiscus*). Blunt-ended electrodes were produced by fire-polishing and have an approximate external tip diameter of 20  $\mu\text{m}$ . The internal tip diameter of the sensor is much smaller and is around 1-2  $\mu\text{m}$ . Scale bar = 100  $\mu\text{m}$ .



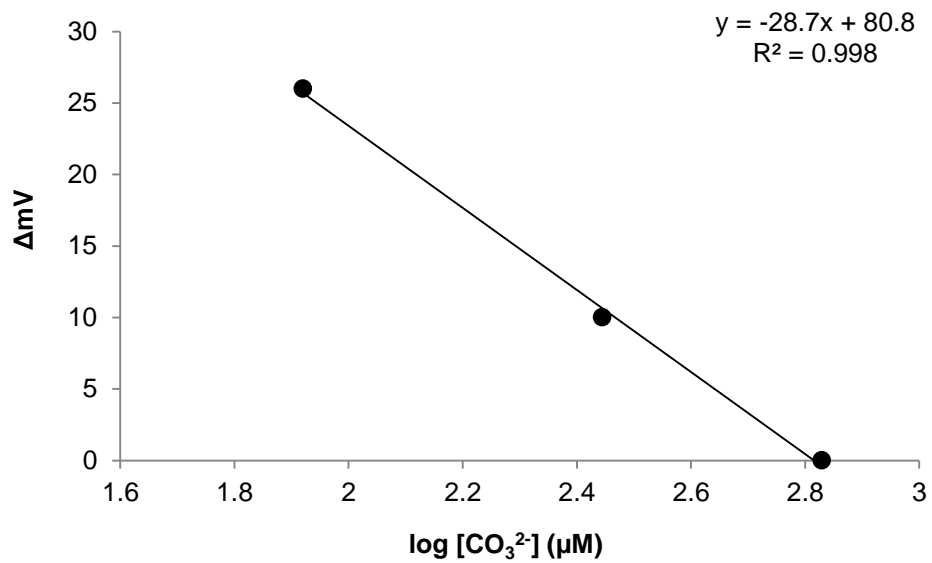
**Supplementary Figure 6: Cellular modelling of carbonate chemistry around a large diatom cell at high CO<sub>2</sub>.**

A-D) Modelled profiles of inorganic carbon species (CO<sub>2</sub>, HCO<sub>3</sub><sup>-</sup>, CO<sub>3</sub><sup>2-</sup>) and pH around a large (r = 60 μm) photosynthesizing cell at high CO<sub>2</sub> (pH = 7.6). The model simulates a cell taking up only CO<sub>2</sub> for photosynthesis. The horizontal axis represents distance away from the cell surface. The results show that even at high CO<sub>2</sub> concentrations eCA activity is required to support the simulated rates of CO<sub>2</sub> uptake. E) Simulated changes in cell surface [CO<sub>3</sub><sup>2-</sup>] for a cell at bulk seawater pH of 7.6, 8.2 or 8.8 (based on the experiment described in Fig. 6). F) Simulated changes in cell surface [H<sup>+</sup>] for a cell at bulk seawater pH of 7.6, 8.2 or 8.8.



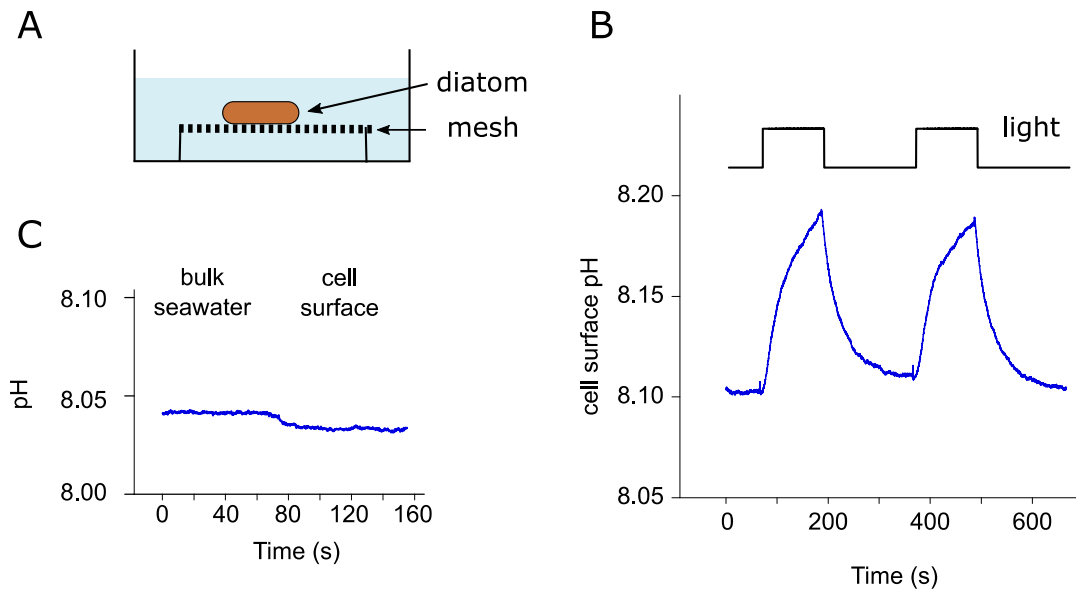
### Supplementary Figure 7: Calibration of pH electrodes

The pH microelectrodes were calibrated using a 3-point calibration using seawater solutions at  $\text{pH}_{\text{NBS}}$  7.0, 8.0 and 9.0. The microelectrode in the example show exhibited a linear response to changes in pH with a slope of -56.9 mV/pH unit.



### Supplementary Figure 8: Calibration of CO<sub>3</sub><sup>2-</sup> microelectrodes

The CO<sub>3</sub><sup>2-</sup> microelectrodes were calibrated using a 3-point calibration. Seawater solutions were adjusted sequentially to pH<sub>NBS</sub> 8.8, 8.2 and 7.6 by bubbling with CO<sub>2</sub>. Seawater pH was monitored continuously during this process using a commercial Ross glass electrode. Samples were taken for total alkalinity (TA) analysis after the pH had stabilised. CO<sub>3</sub><sup>2-</sup> was calculated from pH and TA using CO2SYS. The microelectrode in the example shown exhibited a log-linear response over the range of [CO<sub>3</sub><sup>2-</sup>] examined, with a slope of -28.7 mV/decade.



### Supplementary Figure 9: Support of cells on a fine mesh

To test whether placing cells on directly onto a glass-bottomed dish significantly influenced the formation of the diffusion boundary layer around cells, cell surface pH was also measured around cells that were suspended on a fine mesh (pore size 100  $\mu\text{m}$ ). A) Schematic view of the experimental setup. B) Light-dependent changes in cell surface pH around a single *O. sinensis* cell. Irradiance 100  $\mu\text{mol m}^{-2} \text{s}^{-1}$ . The trace shown is representative of four cells examined. C) Measurement of cell surface pH using a suspended *O. sinensis* cell in the dark compared to bulk seawater. There is a very small decrease in cell surface pH as the microelectrode is positioned against the cell surface. Metabolic processes in the dark therefore only have a minor influence on cell surface pH. A representative trace is shown from three cells examined.